

Predicting Flexural Capacity of Concrete Beams Reinforced with GFRP Bars and Strengthened with CFRP Sheets

M. Talha Junaid¹, Abdalla Elbana¹, Salah Altoubat¹

¹Department of Civil and Environmental Engineering, University of Sharjah
United Arab Emirates

mjunaid@sharjah.ac.ae; U00045867@sharjah.ac.ae; saltoubat@sharjah.ac.ae

Abstract - FRP material has proven to be a proper replacement for the traditional steel reinforcement having superior mechanical properties and high tensile strength. FRP is a highly durable material being nonmagnetic and noncorrosive material. Such materials are effectively used as a construction material that is specially situated in an aggressive environment. This paper investigates the performance of concrete beams reinforced with glass fiber reinforced polymer bars (GFRP) and the applicability of carbon fiber reinforced polymer (CFRP) sheets as a strengthening regime for such systems. With this intent, a total of four 2.4m RC beams were tested. All beams were reinforced with GFRP bars in flexure and shear. Two served as reference beams, and the remaining two were strengthened with CFRP wrap fabric. It was found that the contribution of GFRP bars in load carrying capacity for beams strengthened by CFRP sheet is not as efficient as when CFRP is used with steel rebars. This could be attributed to the difference in stress-strain relationship of the GFRP, CFRP, and steel which are distinctly different from each other. While CFRP and steel have similar modulus values, the modulus value for GFRP is substantially low. Finally, a contribution factor (λ) for predicting the flexural capacity for such systems as per ACI 440 proposal.

Keywords: Glass fiber reinforced polymer, flexural capacity, carbon fiber reinforced polymer, stress-strain; strengthening.

1. Introduction

Conventional steel reinforcement has long been used to provide tensile strength to conventional concrete. However, these are prone to corrosion thus leading to non-durable concrete structures [1]. Recently, fiber-reinforced polymer (FRP) reinforcement bars made of polymer matrices reinforced with glass, carbon, or basalt fibers have become an alternative to the traditional steel reinforcement for concrete [2-4]. FRP has superior durability properties being a nonmagnetic and a noncorrosive material. FRP reinforcement exhibit superior mechanical properties, such as high tensile strength and low self-weight, which make it suitable for concrete structures [5-7]. On the other hand, externally bonded fiber reinforced polymers (FRP) are used for strengthening or repairing of existing concrete members to improve load-resistance as well as serviceability [8]. The fibers are used to create composite sheets which are bonded together by resin. FRP materials are used for strengthening in several forms depending on the application including the flexural and shear strengthening of beams, slabs, columns, and walls. The fibers may be made of carbon, aramid, or glass. Carbon FRP is widely used for strengthening owing to very low creep and high strength and is the most brittle fiber among others. Although the use of Carbon FRP sheets for the strengthening of conventional steel flexural members is widely reported [9-12], the use of glass fiber reinforced polymer bars in flexural members and strengthened with Carbon FRP sheets has not been reported in open literature. This work, therefore, looks at the behavior of the flexural behavior of concrete beams reinforced with GFRP rebars and strengthened with CFRP sheets. The contribution of the reinforcement and strengthening system on the load carrying capacity of such systems is also studied.

2. Materials and Methods

Ordinary Portland cement-based concrete with average compressive strength and modulus of rupture of 41 MPa and 4.05MPa, respectively. Straight GFRP bars without anchor head with a deformed surface under the product name MateenBar provided by Pultron Composites UAE were used in this study. The nominal diameters used were 16 mm for flexural reinforcement ($f_{cu}^* = 690$ MPa $\epsilon_{cu}^* = 0.0135$ and $E_f = 51 \pm 2.5$) and bar size of 10 mm was used for shear reinforcement. All beams were equipped with two 10 mm bars in the compression zone. Four beams, each 2.4m long with a simply supported

span of 2.1m and section of 200mm by 300mm, were tested. The beams were reinforced with 2#16 bars in flexure and #10@70mm in shear and designed to fail in flexure. In the constant moment zone, no stirrups or compression bars were provided, so as not to affect the strain and crack development in the pure bending zone. All beam specimens were tested under four-point bending static test. The load was applied through a spreader beam by a 1500 kN capacity hydraulic jack. The beams were simply supported with a clear span and shear span of 2100 mm and 800 mm, respectively as shown in Fig. 1. The beams were loaded under displacement-controlled loading rate of 0.01 mm/sec. Two beams were loaded to failure. The remaining two beams are loaded to 50% of the experimental ultimate moment to substantially damage them. The damaged beams were repaired by injecting the cracks with epoxy and strengthened with either flat (OPCC-LF) or U wrapped (OPCC-LU) CFRP sheets.

Four strain gauges were installed on the flexural rebars, two at the middle of each shear span (M4, M1) and two at the middle of the clear span (M2, M4). Another four strain gauges were installed at the concrete surface at the midspan section. One at the top surface and three at 20mm, 35mm, and 270 mm depth from the top surface. Fig. 1 shows the location of the 8 strain gauges on GFRP and concrete surface. The CFRP sheets on the strengthened beams were instrumented with four strain gauges, two at mid-span F1 and F2, and one at the half shear span F3. The fourth strain gage (F4) was only mounted on beams with U wrap CFRP strengthening at the side of the beam and at the same depth of the longitudinal reinforcement (Table 1). Linear variable differential transformers (LVDT) were placed beneath the beams' midspan to measure the midspan deflection.

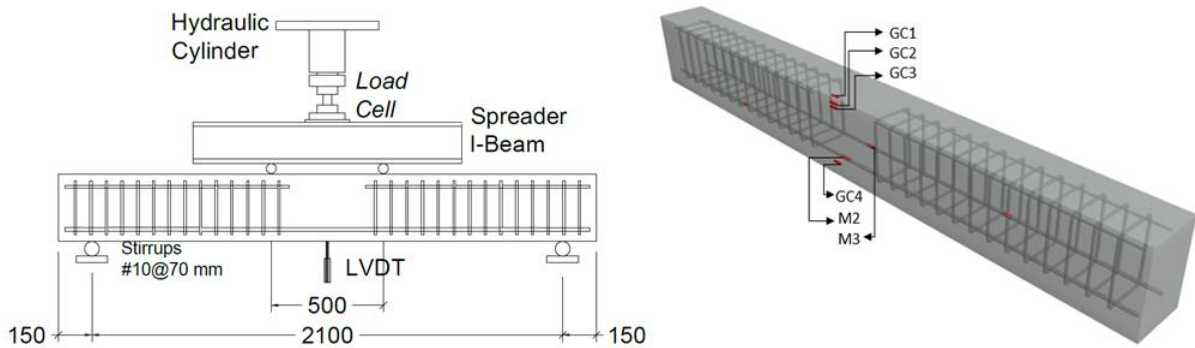


Fig. 1: Schematic diagram of the test set up, beam reinforcement and strain gage location.

Table 1: Beam specimens and strengthening schemes.

Specimen	#CFRP layers	Side View	Side View and CFRP Instrumentation
OPCC-LF	Double		
OPCC-LU	Double		

3. Test results

3.1. Reference Beams

Fig. 2 presents the load-deflection curve of the tested beams. The first phase of the curve for the two reference beams OPCC-R1 and OPCC-R2 is linear up to the load where the beams experienced the first crack. At this point, an average experimental cracking moment $M_{cr,exp}$ of 10.6 kNm is recorded for the beams (Table 2), which translate to a modulus of rupture of 3.6 MPa. The second phase of the curve is nonlinear and less steep because of the reduced stiffness resulting from crack initiation and continues up to the failure point. The observed failure of the reference beams was concrete crushing. After the beams were unloaded, the beams tend to rebound with some residual deflection. This indicates that the GFRP bars did not rupture, and the failure was a ductile failure initiated by concrete crushing as recommended by ACI 440R1. The fact that the maximum strain recorded by the strain gauges M2, and M3 at mid-span of the beams did not exceed the guaranteed rupture strain ($\epsilon_{fu}^* = 1.71\%$) leads to the same conclusion. The average peak flexural capacity (at concrete crushing failure) of the reference beams was 70.6 kNm. Subsequently, the load was removed and the reference beam with GFRP bars rebounded substantially with an average residual deflection of 14.5 mm. The average maximum deflection for the reference beams was 67 mm.

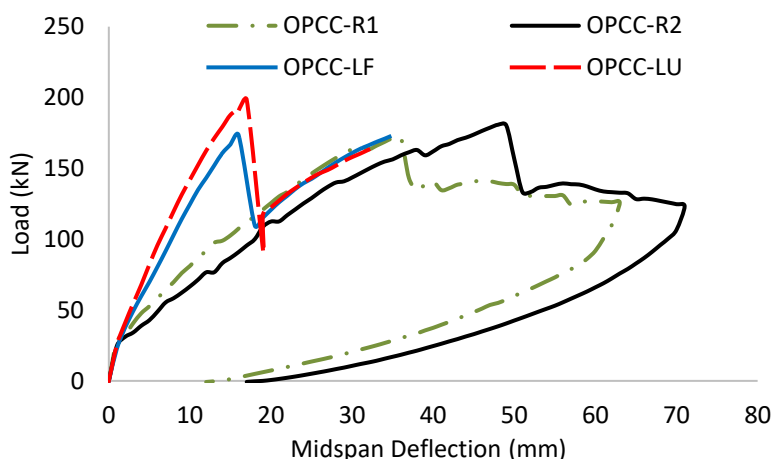


Fig. 2: Load Deflection curve of the tested beams.

3.2. Strengthened Beams

CFRP material is linearly elastic until failure and features a high modulus of elasticity. Accordingly, both OPCC-LF and OPCC-LU beams that were strengthened with CFRP exhibit a relatively steep linear load-deflection relationship up to failure point. The strengthened beams failed due to CFRP rupture beneath the constant moment zone. The rupture failure ensued an abrupt drop in the applied load resistance due to the sudden change in stiffness of the system. However, the beams continued to resist the applied load until the concrete crushing in the compression zone between the applied loads. After CFRP rupture failure, the beam specimen continued to resist applied load and the load-deflection relationship appears to be comparable to the reference beams. Table 2 present the flexural capacity at CFRP rupture ($M_{CFRP,exp}$) and at concrete crushing ($M_{cc,exp}$). The flexural capacity of OPCC-LF and OPCC-LU at CFRP failure changed by -1.4 and +12.2% from its reference beams, while at concrete crushing the change was -0.85 and 5.95%, respectively. As can be seen from the results, the strengthened beams did not substantially undergo a change in the load carrying capacity, although the CFRP increased the stiffness of the beam. Also, the U wrap resulted in higher stiffness compared to the flat sheet beam. The apparent independence of the beam ultimate strength with strengthening a very interesting finding and is discussed in much detail in the next section. At this point, it can be concluded that the increased stiffness of the strengthened beams could be attributed to the higher modulus of elasticity of CFRP sheet compared to GFRP bars which will make the load carrying capacity mostly dependent on the CFRP and will limit the contribution of GFRP rebars. Furthermore, it's worth to mention that the U-shape strengthening technique has effectively improved flexural capacity by 13.5% over the long flat strengthened beam. This may be due to the enhanced anchorage provided by the strengthening system which was able to transfer some of the tensile stresses to the sides.

Table 2: Experimental failure mode and load level at CFRP, GFRP, and concrete crushing.

Specimen	$M_{cr,exp}$	$M_{CFRP,exp}$	$M_{cc,exp}$	Capacity change from R beams		Failure mode
	kNm			At Ultimate Capacity	At concrete crushing	
OPCC- R1	10.0	-	72.4	-	-	Concrete Crushing
OPCC- R2	11.2	-	68.8	-	-	Concrete Crushing
OPCC-LF	10.6	69.6	70.0	-1.4	-0.85	CFRP rupture
OPCC-LU	13.6	79.2	74.8	+12.2	+5.95	CFRP rupture

4. Discussion

4.1. CFRP and GFRP Contribution in flexural strength

Strengthened concrete beams reinforced with conventional steel bars behave differently than beams reinforced with GFRP bars, in such that the steel bars usually yield before CFRP rupture. In such conventional cases after steel yielding, the bars will exhibit plastic behavior and will continue to contribute to load carrying capacity side by side with CFRP sheets.

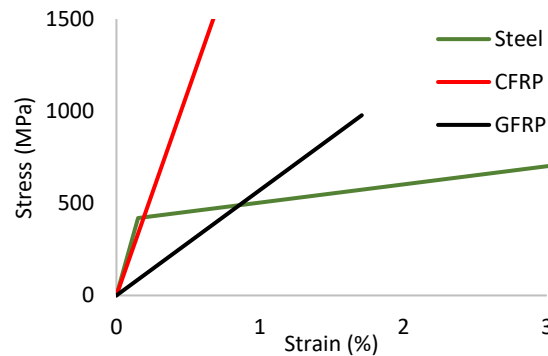


Fig. 3: Typical Stress-strain relationship of steel, GFRP, and CFRP [2].

The strain in CFRP will increase rapidly beyond yielding point of steel until CFRP rupture failure. This will significantly increase the overall load carrying capacity of the strengthened member. However, in case of beams reinforced with GFRP bars and CFRP strengthened, the moment carrying capacity of the beams did not change significantly from the reference beams. The underlying factor is the load carrying mechanism of this composite system. The GFRP bars have a much lower modulus value (51 GPa) than the CFRP sheets (230 GPa) and conventional steel reinforcement (200 GPa), as seen in Fig. 3. This means that for similar strains developed in the two materials, the CFRP will carry substantially higher stresses. This phenomenon leads to the CFRP sheets reaching its capacity while the GFRP bars are not contributing in carrying the load at similar levels. This can be seen clearly in Fig. 4, where the strain measurements in the GFRP bar at mid-span (M2), is comparable to the strain level on CFRP sheets at mid strip soffit (F1 & F2).

4.2. Contribution Factor for GFRP-CFRP Composites

As discussed in the previous section, the load carrying mechanism for CFRP-GFRP composite concrete beams is very different from CFRP and conventional steel. It is therefore imperative that this is reflected in the capacity equation for finding the ultimate moment of such flexural members. This section attempts to develop such a factor based on the experimental results discussed here.

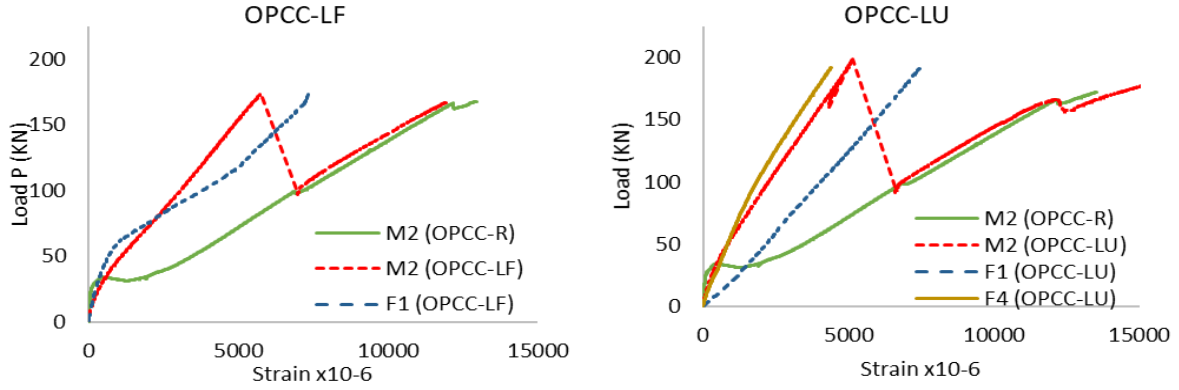


Fig. 4: Strain distribution in CFRP (F1,4) and GFRP rebars (M2) in reference beams and strengthened beams.

Equation (1-3) from ACI 440.R2-08 to calculate the nominal flexural strength of RC beam reinforced with tradition steel rebars and strengthened with FRP is as follow:

Steel rebars contribution to bending:

$$M_{n,s} = A_s f_s \left(d - \frac{\beta_1 c}{2} \right) \quad (1)$$

FRP contribution to bending:

$$M_{n,CFRP} = A_f f_{fe} \left(d_{fe} - \frac{\beta_1 c}{2} \right) \quad (2)$$

The overall contribution of nominal strength is as follows:

$$M_n = M_{n,s} + \psi M_{n,f} \quad (3)$$

Where, ψ is the reduction factor on the contribution of FRP to beam strength due to uncertainties in the FRP composite system. The code recommends a value of 0.85 for this reduction factor. In the above equations, the coefficient β_1 is defined based on concrete strength in ACI 440.R2, c is the depth of the neutral axis A_s and A_f are the reinforcement area of steel and the external FRP reinforcement respectively, d and d_{fe} are the reinforcement depth and FRP depth from the top surface, respectively, and lastly f_s and f_{fe} is the stress level in steel and external FRP, respectively. In case of over-reinforced beams with GFRP bars equation 1 from ACI 440.R2 should be replaced by ACI440.R1-06 equation (4) to calculate the GFRP rebars contribution to bending capacity:

$$M_{n,GFRP} = \rho_f f_f \left(1 - 0.59 \frac{\rho_f f_f}{f'_c} \right) b d^2 \quad (4)$$

Where, ρ_f is the reinforcement ratio, f_f is the stress is GFRP bars, b is the width of the section and d is the distance from the extreme compression to the centroid of the tension reinforcement. As can be seen from Fig. 3, the CFRP and steel have similar modulus values, while the modulus value for GFRP is much lower. This is reflected in the performance of the two materials working in tandem in flexure as discussed in the previous section. Therefore, any moment capacity prediction equation must not simply be an algebraic sum of the independent moment capacities as in case of steel-FRP systems. The newly proposed equation would be of the following form:

$$M_n = \lambda M_{n,GFRP} + \psi M_{n,CFRP} \quad (5)$$

Where, λ is the contribution factor applied to the moment capacity contribution of GFRP bars. Fig. 4 present the load-strain graph at GFRP rebars (strain gauges M2 at mid-span) for both control beams and strengthened beams. The graphs show that at the same load levels, GFRP strain of control beams is much higher than the GFRP strain in the CFRP strengthened beams. Therefore, the contribution factor λ could be approximated by finding the ratio of the strain level of GFRP bars between control and strengthened beams at an equivalent load level. This determination can provide an estimate of the load at which a certain strain was achieved in the reference and strengthened beams. Hence the contribution factor λ could be defined as follow:

$$\lambda = \frac{\varepsilon_{u1,GFRP}}{\varepsilon_{u0,GFRP}} \quad (6)$$

Where, $\varepsilon_{u0,GFRP}$ is the strain of GFRP bars without CFRP strengthening and $\varepsilon_{u1,GFRP}$ is the strain of GFRP bars with CFRP strengthened beams at an equivalent applied load. Table 3 summarizes the computed contribution factors at different load levels for the tested beams in this research.

Table 3: Computed contribution factor.

Specimen	$\varepsilon_{u1,gfrp}$	$\varepsilon_{u0,gfrp}$	$\varepsilon_{u1,gfrp}$	$\varepsilon_{u0,GFRP}$	$\varepsilon_{u1,gfrp}$	$\varepsilon_{u0,gfrp}$	λ_{50}	λ_{85}	$\lambda_{fail.}$
	At 50KN		At 85KN		At failure				
OPCC-LF	1086	2733	2480	6024	5781	13865	0.40	0.41	0.42
OPCC-LU	841	2733	1663	6024	5145	14272	0.31	0.28	0.36

Table 4: Accuracy of theoretical and experimental flexural capacity.

Specimen	$M_{n,GFRP,theo}$	$M_{n,CFRP,theo}$	$M_{n, ACI440.R2}$	$M_{n, proposed}$	$M_{n,exp}$	$M_{n,tho} / M_{n,exp}$	$M_{n,propose} / M_{n,exp}$
	ACI	ACI	Equation 3	Equation 5			
	440.R01(4)	440.R02 (2)	a	b			
OPCC-LF	48.5	46.7	88.2	58.04	69.6	1.27	0.83
OPCC-LU	48.5	63.6	102.6	64.12	79.2	1.30	0.81

The proposed contribution factor is verified by computing the theoretical flexural capacity from the proposed equation 5 and comparing it with the observed experimental flexural capacity and the recommended equation from ACI 440-R02. These are tabulated in Table 4. The proposed equation with an additional contribution factor for the GFRP contribution gives good agreement with the experimental results. In these cases, the predicted capacity is lower than the actual experimental values. Also, worth noting is that ACI 440-R02 prediction for these cases is always higher than the actual capacities.

5. Conclusion

Based on the results and observations of the experiments conducted, the following conclusions can be drawn:

- The load carrying mechanism of the GFRP-CFRP concrete system is very different from the Steel-CFRP system. This is due to the fact that the GFRP bars have a much lower modulus value than the CFRP sheets. However, for such systems, the original capacity of the beams is restored.
- Based on initial results it appears that the ACI 440R2 flexural capacity estimation of GFRP-CFRP system is not conservative. It is therefore recommended that more work on this aspect be undertaken and a reduction factor be proposed based on such a study. Currently, a reduction factor is proposed here and gives good agreement with experimental results using the well-established ACI 440 R2 methodology.

Acknowledgements

The authors would like to acknowledge the support provided by the Sustainable Construction Materials and Structural Systems (SCMASS) research group at the University of Sharjah. The research was funded by research grant number 1602040128-P, provided by the University of Sharjah. Support provided by Pultron Composites and Conmix Ltd. is also highly appreciated.

References

- [1] ACI 318-08, "Building code requirements for structural concrete and commentary," *American Concrete Institute*, 2008
- [2] ACI 440.1R-06, "Guide for the design and construction of structural concrete reinforced with FRP bars," *American Concrete Institute*, 2006.
- [3] A. Elbana, M. T. Junaaid, S. Altoubat, "Flexural behavior and strengthening of geopolymer concrete beams reinforced with GFRP bars using CFRP sheets," in *SynerCrete'18 International Conference on Interdisciplinary Approaches for Cement-based Materials and Structural Concrete*, Funchal, Madeira Island, Portugal, 2018, pp. 449-454.
- [4] A. Elbana, "Evaluation of flexural behavior of reinforced concrete beams with glass fiber reinforced polymer (GFRP) bars," M.Sc. Thesis, Dept. of Civil and Envr. Eng., University of Sharjah, 2018.
- [5] H. Toutanji, and M. Saafi, "Flexural behavior of concrete beams reinforced with glass fiber-reinforced polymer (GFRP) bars," *ACI Struct. J.*, vol. 97, no. 5, pp. 712-719, 2000.
- [6] S. H. Alsayed, "Flexural behaviour of concrete beams reinforced with GFRP bars," *Cement Concrete Comp.*, vol. 20, no. 1, pp. 1-11, 1998.
- [7] E. G. Nawy, and G. E. Neuwerth, "Fiberglass reinforced concrete slabs and beams," *J. Struct. Div. ASCE*, vol. 103 no. 2, pp. 421-440, 1977.
- [8] K. Soudki and T. Alkhrdaji, "Guide for the design and construction of externally bonded FRP systems for strengthening concrete structures (ACI 440.2 R-02)," in *Structures Congress*, 2005, pp. 1-8.
- [9] U. Meier, and H. Kaiser, "Strengthening of structures with CFRP laminates," *Adv. Comp. Mat. in Civil Eng. Struct. ASCE*, 1991.
- [10] T. Norris, H. Saadatmanesh, and M. Ehsani, "Improving the serviceability of concrete beams using carbon fiber reinforced polymer (CFRP) sheets," *Fed. Highway Admin.*, 1994.
- [11] I. M'Bazaa, M. Missihoun, and P. Labossiere, "Strengthening of reinforced concrete beams with CFRP sheets," in *First International Conference on Composites in Infrastructure*, pp. 746-759, 1996.
- [12] M. Shahawy, M. Arockiasamy, T. Beitelman, R. Sowrirajan, "Reinforced concrete rectangular beams strengthened with CFRP laminates," *Comp. Part B: Eng.*, vol. 27, no. 3, pp. 225-233, 1996.